

000  
001  
002  
003  
004  
005  
006  
007  
008  
009  
010  
011  
012  
013  
014  
015  
016  
017  
018  
019  
020  
021  
022  
023  
024  
025  
026  
027  
028  
029  
030  
031  
032  
033  
034  
035  
036  
037  
038  
039  
040  
041  
042  
043  
044  
045  
046  
047  
048  
049  
050  
051  
052  
053

054  
055  
056  
057  
058  
059  
060  
061  
062  
063  
064  
065  
066  
067  
068  
069  
070  
071  
072  
073  
074  
075  
076  
077  
078  
079  
080  
081  
082  
083  
084  
085  
086  
087  
088  
089  
090  
091  
092  
093  
094  
095  
096  
097  
098  
099  
100  
101  
102  
103  
104  
105  
106  
107

# Improving Face Recognition from Caption Supervision with Multi-Granular Contextual Feature Aggregation

Anonymous IJCB 2023 submission

## Abstract

We introduce caption-guided face recognition (CGFR) as a new framework to improve the performance of commercial-off-the-shelf (COTS) face recognition (FR) systems. In contrast to combining soft biometrics (e.g., facial marks, gender, and age) with face images, in this work, we use facial descriptions provided by face examiners as a piece of auxiliary information. However, due to the heterogeneity of the modalities, improving the performance by directly fusing the textual and facial features is very challenging, as both lie in different embedding spaces. In this paper, we propose a contextual feature aggregation module (CFAM) that addresses this issue by effectively exploiting the fine-grained word-region interaction and global image-caption association. Specifically, CFAM adopts a self-attention and a cross-attention scheme for improving the intra-modality and inter-modality relationship between the image and textual features. Additionally, we design a textual feature refinement module (TFRM) that refines the textual features of the pre-trained BERT encoder by updating the contextual embeddings. This module enhances the discriminative power of textual features with a cross-modal projection loss and realigns the word and caption embeddings with visual features by incorporating a visual-semantic alignment loss. We implemented the proposed CGFR framework on two face recognition models (ArcFace and AdaFace) and evaluated its performance on the Multimodal CelebA-HQ dataset. Our framework improves the performance of ArcFace from 16.75% to 66.83% on  $TPR@FPR=1e-4$  in the 1:1 verification protocol.

## 1. Introduction

Despite remarkable advancements in face recognition due to the adoption of margin-based loss functions [2, 14], face recognition in unconstrained scenarios remains a challenging problem [38]. The presence of covariate factors in an unconstrained environment, such as resolution, illumination, and pose, affects the face image quality, thus, de-

creasing the recognition performance. Providing auxiliary information, such as facial marks, gender, ethnicity, age, and skin color, to a face recognition (FR) system can improve its recognition performance [5, 39]. For example, in an unconstrained environment such as video surveillance, where a prevalent commercially-off-the-shelf (COTS) system performs poorly [38, 41], the application of soft biometrics has been proven to improve the performance of hard biometrics [30, 5].

Natural language captions that describe the visual contents of a face are an essential soft biometric trait for face recognition. In this study, we will explore whether we can boost the performance of a FR system using caption supervision. Our caption-guided face recognition (CGFR) has enormous potential in various applications, such as criminal and intelligence investigation, video surveillance, etc. For example, using a CGFR model, law-enforcement agencies can quickly retrieve the suspect face from a low-quality CCTV footage and a short description of eyewitnesses.

Although captions are rich, they face many challenges that limit their application in the biometric system. As natural language contains high-dimensional information, it is often much more abstract than images. A short textual description of a given face consisting of a few sentences is insufficient to describe all the minute details of the facial features. Consequently, CGFR is significantly different from other tasks such as cross-modal image-text retrieval (ITR) [13, 17] and image-text matching (ITM) [16], where the matching text has a description of the various objects, background scenes, styles, etc. Moreover, different people may have different captions for a particular face.

To improve the performance of the FR systems using CGFR, it is essential to find not only the semantic understanding of textual contents but also the proper association between visual and textual modalities. This is because the embedding space of images and text lies in different spaces due to the heterogeneity of the two modalities [17]. Aligning the image features with word embeddings is thus crucial, as it has a significant impact on the performance of a cross-modal fusion algorithm [17]. In this work, we fine-tune the state-of-the-art BERT model [4] to update the con-

108 textual associations among words in the caption by incorporating a visual-semantic alignment loss [36] and a cross-  
 109 modal classification loss [40]. Finetuning the text encoder is  
 110 essential because the BERT model was trained with different  
 111 objectives than ours. Therefore, we finetune to achieve  
 112 two objectives: (1) to learn visually aligned text embedding,  
 113 i.e., to realign word and caption embeddings with visual in-  
 114 formation, and (2) to enhance the discriminative power of  
 115 textual features.  
 116

117 However, a simple feature-level cross-modal fusion  
 118 without fine-grained interaction between image-text tokens  
 119 does not perform well. Therefore, we propose a novel  
 120 module, namely, contextual feature aggregation module  
 121 (CFAM), to effectively carry out the fine-grained word-  
 122 region interaction and global image-caption association on  
 123 two different granularities. There are mainly three net-  
 124 works in the proposed CFAM: caption-level context mod-  
 125 eling, word-level context modeling, and a feature ag-  
 126 gregation network. Both context modeling networks adopt a  
 127 self-attention and a cross-attention mechanism. The self-  
 128 attention mechanism increases the intra-modality relation-  
 129 ship within each modality, while the cross-attention mech-  
 130 anism improves the inter-modality relationship between im-  
 131 age and textual features. The inputs to the feature ag-  
 132 gregation network are the context-enhanced features from the  
 133 word and caption level context modeling.  
 134

135 We conduct our experiments on a benchmark text-to-  
 136 face dataset, namely, Multi-Modal CelebA-HQ [33] (MM-  
 137 CelebA). Sample image-caption pairs of the dataset are il-  
 138 lustrated in Figure 1. In fact, the dataset is based on a sub-  
 139 set of the CelebA dataset [21] that contains high-resolution  
 140 images with very low variation. In our experiment, we re-  
 141 move the crucial face-alignment step and apply some pre-  
 142 processing steps such as random sub-sampling, rotation,  
 143 flip, etc., to augment our database as well as downgrade  
 144 the image quality in order to mimic real-world low qual-  
 145 ity video surveillance scenarios. The verification rate of FR  
 146 systems, such as ArcFace [2] and AdaFace [14], drops dras-  
 147 tically on this preprocessed dataset because the images are  
 148 corrupted with down-sampling and noise, which adversely  
 149 affect their facial analysis procedure [41]. We then apply  
 150 our CGFR framework to both systems. The experimental  
 151 results demonstrate a remarkable performance leap over the  
 152 COTS systems.  
 153

154 In this study our contributions are: (1) exploring a new  
 155 paradigm to improve face recognition with natural language  
 156 supervision, (2) proposing the CFAM module to exploit  
 157 fine-grained interaction among local and global features us-  
 158 ing word and caption-level of granularity, (3) designing a  
 159 textual feature refinement module (TFRM) to refine textual  
 160 features and align them with visual content by fine-tuning  
 161 the BERT encoder, and (4) conducting extensive experi-  
 162 ments on the MMCelebA [33] dataset using the proposed

Input Caption	Preprocessed Images	162
This attractive person has sideburns, bushy eyebrows, mustache, big nose, goatee, and oval face.		163
This man has wavy hair, oval face, mustache, bushy eyebrows, sideburns, bags under eyes, and big nose.		164
This woman has mouth slightly open. She is attractive, and young and is wearing heavy makeup.		165
The person has big lips, wavy hair, arched eyebrows, high cheekbones, bags under eyes, brown hair, and pointy nose. She is wearing lipstick.		166

167 Figure 1. Sample image-caption pairs from the state-of-the-art  
 168 Multi-Modal CelebA-HQ text-to-face dataset.  
 169

170 CGFR framework to demonstrate substantial improvements  
 171 over existing FR systems. Finally, this work demonstrates  
 172 excellent potential for caption-guided face recognition and  
 173 provides a promising approach for further research.  
 174

175 The rest of this paper is organized as follows: an  
 176 overview of the related works is presented in Section 2. A  
 177 detailed description of the proposed method, including steps  
 178 to finetune the BERT encoder, is presented in Section 3. In  
 179 Section 4, we demonstrate the experimental evaluation of  
 180 the CGFR framework. Finally, we summarize our results  
 181 with some possible future research directions in Section 5.  
 182

## 2. Related Work

### 2.1. Soft Biometrics

183 Facial semantic attributes, such as facial marks, hair  
 184 color, gender, ethnicity, age, and skin color, have been sig-  
 185 nificantly exploited as auxiliary information to improve the  
 186 performance of tasks such as face image retrieval and face  
 187 verification. However, most of the prior works in the liter-  
 188 ature on improving face recognition using soft biometrics  
 189 have been based on using categorical labels [5, 39]. Zhang  
 190 *et al.* [39] integrated a set of five soft biometrics (ethnic-  
 191 ity, gender, eyebrow, eye color, and hair color) with hard  
 192 biometric systems. Compared to the baseline recogni-  
 193 tion rates at  $\text{FAR} = 0.001$ , their verification rate improved up to  
 194 15.5% when introducing all the soft biometrics and 16.4%  
 195 when introducing gender information on the ugly part of  
 196 the GBU database. Furthermore, authors in [5] empirically  
 197 proved that a manual estimation of the six most discrimina-  
 198 tive soft biometric improves the relative performance of the  
 199 FR systems (COTS Face++ and VGG-face) up to 40% over  
 200 the LFW database.  
 201

### 2.2. Caption-Guided Face Recognition

202 Several early works have been proposed for caption-  
 203 supervised face recognition [11, 7]. Huang *et al.* [11] im-  
 204 proved state-of-the-art face recognition using web-scale im-  
 205 ages.  
 206

216 ages with captions by learning the feature space in an iterative  
 217 label expansion process. However, they only employed  
 218 captions to extrapolate the labels of the face identity.  
 219

220 Recently, with the development of generative adversarial  
 221 networks (GANs) [6] and transformers [31], text-to-face  
 222 synthesis [32, 29], and facial attribute editing [9, 33] with  
 223 textual descriptions have gained increasing popularity. For  
 224 example, TediGAN [33] uses latent code optimization of  
 225 pre-trained StyleGAN for caption-guided facial image  
 226 generation and manipulation. In contrast to these works, we  
 227 introduce a new line of research by exploring the idea of using  
 228 natural language captions to improve the performance of the  
 229 FR systems. As there are no publicly available datasets that  
 230 contain large-scale image-caption pairs for our task, we  
 231 employ MMCelebA [33] dataset which has been widely used  
 232 for text-to-face synthesis.

### 233 2.3. Attention Techniques

234 Recently, different attention mechanisms, such as self-  
 235 attention, cross-attention, etc., have been extensively ex-  
 236 ploited in various multimodal tasks [18, 16, 36, 37]. Cross-  
 237 attention or co-attention is an attention mechanism initially  
 238 proposed in transformers [31] that interacts with two em-  
 239 bedding sequences from different modalities (e.g., text, im-  
 240 age). Li *et al.* [18] propose a latent co-attention mecha-  
 241 nism in which spatial attention relates each word to corre-  
 242 sponding image regions. Also, Lee *et al.* [16] developed a  
 243 stacked cross-attention network that learns the cross-modal  
 244 alignments among all regions in an image and words in a  
 245 sentence. Xu *et al.* [36] applied an attention mechanism to  
 246 guide the generator to focus on different words while gen-  
 247 erating various image sub-regions. They also proposed a  
 248 deep attentional multimodal similarity model (DAMSM) to  
 249 improve the similarity between the generated images and  
 250 the given descriptions. To re-weight the importance of local  
 251 image regions in tasks such as image synthesis [36], image  
 252 caption generation [35], image segmentation [28, 37], and  
 253 image-text matching [16, 18], word-level attention has been  
 254 employed. However, only employing word-level attention  
 255 cannot ensure global semantic consistency due to the di-  
 256 versity of the text and image modalities. Global contextual  
 257 information is also important as it provides more informa-  
 258 tion on the visual content of the image, and context of the  
 259 caption. Therefore, global image-caption attention should  
 260 also be considered to drive the global features toward a  
 261 semantically well-aligned context.

### 262 2.4. Multimodal Representation Learning

263 In recent years, dual-stream approaches, where the im-  
 264 age and text encoder are trained on large-scale datasets  
 265 individually with different cross-modality loss functions,  
 266 have become widely popular in tackling various multimodal  
 267 downstream tasks [25]. A lot of cross-modal loss functions

268 such as contrastive [25, 19], triplet [16], word-region align-  
 269 ment [36], cross-modal projection [40], etc., have been pro-  
 270 posed as part of the training objectives. Zhang *et al.* [40]  
 271 proposed a novel projection loss that consists of two losses:  
 272 a cross-modal projection matching (CMPM) loss for com-  
 273 puting the similarity between image-text pairs and a cross-  
 274 modal projection classification (CMPC) loss for learning  
 275 a more discriminative visual-semantic embedding space.  
 276 However, most of the dual-stream approaches in the lit-  
 277 erature cannot effectively and accurately exploit the fine-  
 278 grained interaction among word-region features.  
 279

280 Furthermore, other researchers [37] has used image and  
 281 textual features, extracted from separate encoders, which  
 282 are often concatenated to be fed into a fusion module  
 283 to learn joint representations. However, a simple fusion  
 284 scheme may not be effective since the unaligned visual  
 285 and word tokens lack prior relationships. Therefore, cross-  
 286 modal interaction from local and global contexts is essen-  
 287 tial to improve multimodal fusion performance. For exam-  
 288 ple, Niu *et al.* [24] map phrases-region and image-caption  
 289 into a joint embedding space using an image-text alignment  
 290 method that consists of three different granularities: global-  
 291 global alignment, global-local alignment, and local-local  
 292 alignment.

293 In this work, we adopt a dual-stream approach to  
 294 extract facial and textual features from pre-trained en-  
 295 coders. We use a visual semantic alignment loss, known as  
 296 DAMSM [36], to align the visual and word tokens locally  
 297 and globally. We also employ CMPC loss [40] to enhance  
 298 the discriminative power of the features. Finally, for fine-  
 299 grained cross-modal interaction, we design CFAM.

## 3. Framework

300 An overview of our proposed framework is depicted in  
 301 Figure 2. The framework comprises three modules: a fea-  
 302 ture extraction module consisting of an ArcFace FR mod-  
 303 ule, a contextual feature aggregation module, CFAM, and a  
 304 refined pre-trained text encoder, TFRM.

### 305 3.1. Facial Feature Extraction

306 We first employ the ArcFace model [2] as a feature ex-  
 307 tractor to extract the facial features from the input image.  
 308 Specifically, we choose ResNet18-IR [8, 2] for the back-  
 309 bone of the ArcFace model, which was pre-trained on the  
 310 MS1MV3 dataset [3]. Here, we modify the ResNet18-IR  
 311 architecture by replacing the global average-pooling layer  
 312 with a fully connected layer. The output of the fully con-  
 313 nected layer is a 512-dimensional feature vector, which is  
 314 considered as the global features  $\mathbf{v} \in \mathbb{R}^{512}$  of the input im-  
 315 age, as it contains high-level visual information. We extract  
 316 the local features of the image  $I \in \mathbb{R}^{256 \times 14 \times 14}$  from the  
 317 output of the third IR block. The size of the input image is  
 318  $3 \times 112 \times 112$ . We further employ CGFR on the AdaFace  
 319

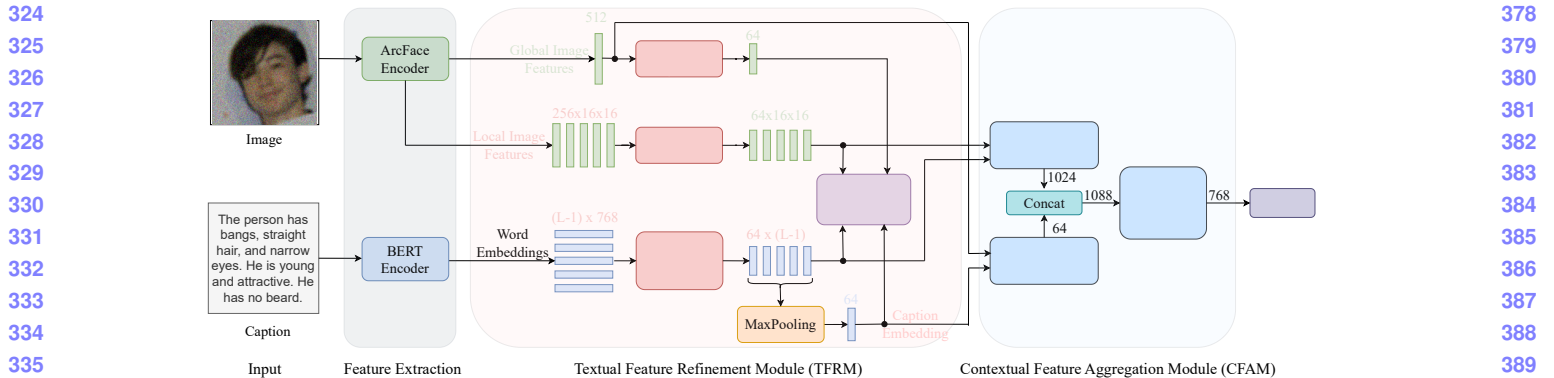


Figure 2. An overview of our proposed CGFR framework: it contains an ArcFace FR module and a pre-trained text encoder for extracting the facial features and textual embeddings from the input image-caption pair, respectively. First, TFRM updates contextual associations of the text embedding by finetuning the text encoder using the state-of-the-art DAMSM loss [36] and a cross-modal projection loss [40]. Next, CFAM fuses the facial features with textual embeddings through cross-attention at both the word and caption-level of granularities.

model [14]. Here, the backbone ResNet18-IR is similar to the ArcFace model; however, it was pre-trained on the WebFace4M dataset [42]. In contrast to ArcFace, the input is a BGR image.

### 3.2. Textual Feature Extraction

#### 3.2.1 BiLSTM

Most of the works in the literature usually employ a long short-term memory network (LSTM) [10] as an encoder to extract text embeddings from natural language descriptions [35, 36]. Therefore, in this work, as a baseline, we use a bidirectional LSTM (BiLSTM) [27] as a text encoder to extract semantic vectors from the input captions. The BiLSTM encoder encodes the input caption as a matrix of  $W \in \mathbb{R}^{L \times D}$ . Here,  $D$  denotes the dimension of the word vector, and  $L$  denotes the maximum number of words in a caption. In our experiment, for the BiLSTM encoder, we consider a maximum of 18 words per caption, and the dimension of the word embedding is 256. Therefore, for an input caption of  $L$  words, the word embeddings are  $[w_1, w_2, \dots, w_L]$ , where  $w_L \in \mathbb{R}^D$  is the caption embedding.

#### 3.2.2 BERT

One of the limitations of traditional word embedding (such as word2vec) is that they only have one context-independent embedding for each word. Devlin *et al.* [4] introduced BERT, a deep bidirectional encoder that considers the context of a word for each occurrence. In this work, we adopt a pre-trained BERT-base model with 12 encoder layers, each having 12 attention heads. It obtains the contextual embedding of each word by exploiting all the words in the caption. Furthermore, in addition to the input tokens, we add a [CLS] token at the beginning and a [SEP] token at the end of each sentence in the caption. The maximum length of the

token sequence,  $L$ , is set to 21. Additional [PAD] tokens are added for short-length captions after the last [SEP] token. Extra tokens are truncated if the length of the input tokens is higher than  $L$ . Therefore, the input to the BERT-base model looks like this:

[CLS],  $w_2, w_3, \dots, w_{L-3}, [SEP], [PAD], [PAD], \dots$

The output of the BERT layer gives a word matrix,  $W \in \mathbb{R}^{L \times 768}$ , where each contextualized token has an embedding of 768 dimensions. Here, the first token, [CLS], is a classification token that represents the global embedding of the caption. The remaining  $L - 1$  tokens represent the contextualized word embeddings. In addition to BERT-base, we also experimented with other variants of BERT such as BERT-large, DistilBERT-base [26], and RoBERTa-base [20]. However, in our experiments, we found that the performance of these variants is almost the same.

### 3.3. Textual Feature Refinement Module

In this subsection, we briefly describe the proposed textual feature refinement module (TFRM). Because our text encoder was pre-trained with objectives that are totally different from ours and it creates embeddings that are unaligned to the image features, we need to refine the textual features. We design TFRM to realign the word and caption embedding with visual information. As shown in Figure 2, our TFRM consists of a convolution-based projection for text embeddings, a projection head for local image features, and a module to implement the visual-semantic alignment loss, DAMSM, and a cross-modal projection classification loss.

#### 3.3.1 Projection Heads

**Convolution-based Projection:** As a caption has a natural order of word sequences, it is useful to extract not only

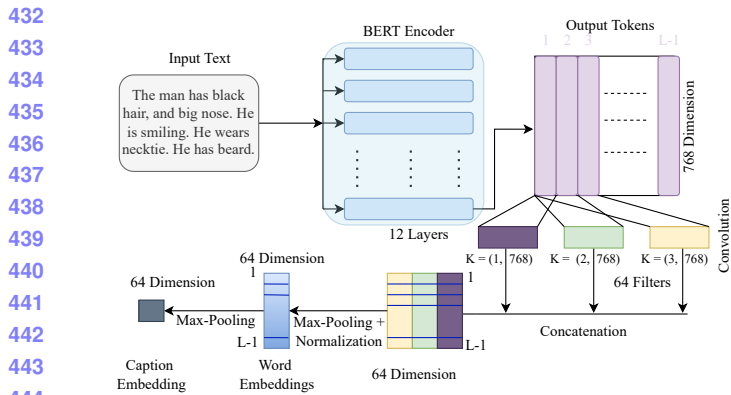


Figure 3. The proposed convolution-based projection for creating the word embeddings and global embedding for the caption. 2D-convolutions with three different kernel sizes are applied to the output representations of the BERT encoder to extract both the word- and phrase-level information.

word-level features but also phrase-level features. Thus, we apply a 2D-convolution to the output of the BERT sequence to extract both word-level and phrase-level information from the input caption. The first dimension of the kernel size  $K$  is set to 1, 2, and 3 to project uni-gram, bi-gram, and tri-gram word sequences, respectively. For  $K = 2$  and 3, the word representations,  $W$ , are appropriately padded to maintain the fixed length of the sequence. All of these convolutions have a total of 64 filters with a stride of 1. Next, we apply the max-pooling operation followed by an  $L_2$  normalization across the outputs of the convolutions to generate the word embeddings,  $\mathbb{R}^{(L-1) \times 64}$ . Figure 3 illustrates the proposed scheme for creating word embeddings from the output of BERT encoder.

**Caption Embedding:** There are multiple ways of creating the global embedding for the input caption,  $\mathbf{c} \in \mathbb{R}^{64}$ . One common way to create caption embedding is to employ a linear projection followed by a batch normalization [12] on the  $[CLS]$  token of the BERT output layer. We can also create the caption embedding by applying the max-pooling operation across the word embeddings of the convolution-based projection followed by an  $L_2$  normalization. However, we achieved better results from the embeddings which was created by the later scheme. Figure 3 also depicts the scheme.

**Projection Head for Image Features:** We need to project the local image features  $I$ , into 64 dimension which is the optimal dimension of the word embeddings. So, we design a projection head which consists of a  $1 \times 1$  convolution with 64 filters and a Leaky ReLU [34] for non-linearity.

### 3.3.2 Objective Function

**DAMSM Loss:** AttnGAN [36] introduced DAMSM loss to align image-caption pair by using word-level and caption-level attention. Let  $(W, I)$  denote an image-caption pair, where  $W \in \mathbb{R}^{L \times D}$  represents the word embeddings, and  $I \in \mathbb{R}^{H \times W \times D}$  represents the transposed local image features. Then, we apply DAMSM loss [36] to perform cross-modal contrastive learning between image-caption pair. The loss actually minimizes the negative log posterior probability of the similarity scores between the image-caption pair.

**Cross-Modal Projection Classification Loss:** In order to produce discriminative textual features, we also apply a cross-modal projection classification (CMPC) [40] loss. This loss first tries to project the representations from one modality onto the corresponding features from another modality and then classify them using normalized softmax loss. The input to the CMPC is the global image features,  $\mathbf{v}$ , and caption embeddings,  $\mathbf{c}$ . First, the image features are projected onto the normalized text embeddings,  $\bar{\mathbf{c}}$ . Therefore, the normalized softmax loss for the image features,  $L_{ipt}$ , is given by:

$$L_{ipt} = \frac{1}{N} \sum_i -\log\left(\frac{\exp(W_{yi}^T \hat{\mathbf{v}}_i)}{\sum_j \exp(W_j^T \hat{\mathbf{v}}_i)}\right). \quad (1)$$

Here,  $\hat{\mathbf{v}}_i = \mathbf{v}_i^T \bar{\mathbf{c}}_i \bar{\mathbf{c}}_i$  denotes the vector projection of the image features. Now, let's project the text embeddings onto the normalized image features,  $\bar{\mathbf{v}}$ . Therefore, the text classification loss function,  $L_{tpi}$ , is given by:

$$L_{tpi} = \frac{1}{N} \sum_i -\log\left(\frac{\exp(W_{yi}^T \hat{\mathbf{c}}_i)}{\sum_j \exp(W_j^T \hat{\mathbf{c}}_i)}\right). \quad (2)$$

Here,  $\hat{\mathbf{c}}_i = \mathbf{c}_i^T \bar{\mathbf{v}}_i \bar{\mathbf{v}}_i$  denotes the vector projection of the textual features. The total CMPC loss is the summation of the two losses, as defined by Eq. 1 and Eq. 2.

**Full Objective:** Our overall loss function is the weighted combination of the DAMSM and CMPC losses:

$$L_{loss} = \lambda_1 L_{DAMSM} + \lambda_2 L_{CMPC} \quad (3)$$

where,  $\lambda_1$  and  $\lambda_2$  are the hyperparameters that control the DAMSM and CMPC losses, respectively.

### 3.4. Contextual Feature Aggregation Module

Recent works suggest that introducing global image-caption associations in addition to fine-grained word-region interaction can lead to a more effective cross-modal fusion [24]. Therefore, it is equally important to enforce both

432  
433  
434  
435  
436  
437  
438  
439  
440  
441  
442  
443  
444  
445  
446  
447  
448  
449  
450  
451  
452  
453  
454  
455  
456  
457  
458  
459  
460  
461  
462  
463  
464  
465  
466  
467  
468  
469  
470  
471  
472  
473  
474  
475  
476  
477  
478  
479  
480  
481  
482  
483  
484  
485

486  
487  
488  
489  
490  
491  
492  
493  
494  
495  
496  
497  
498  
499  
500  
501  
502  
503  
504  
505  
506  
507  
508  
509  
510  
511  
512  
513  
514  
515  
516  
517  
518  
519  
520  
521  
522  
523  
524  
525  
526  
527  
528  
529  
530  
531  
532  
533  
534  
535  
536  
537  
538  
539

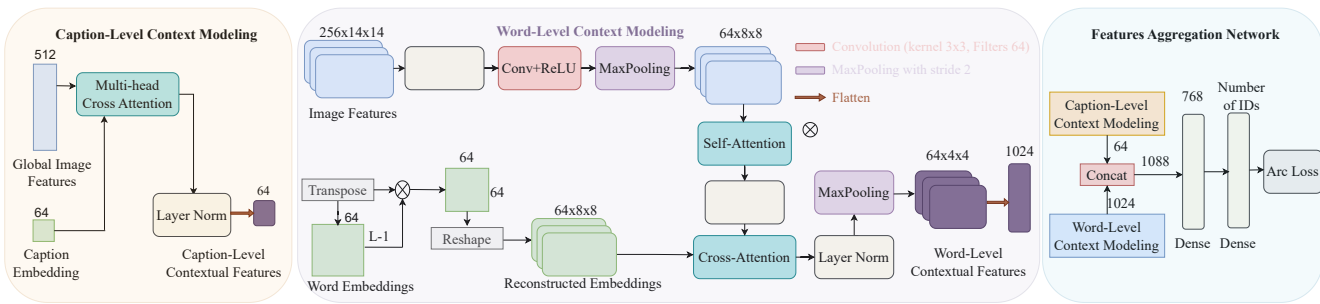


Figure 4. The block diagram of the proposed contextual feature aggregation module. It applies cross-modal feature interaction on both word and caption levels using an attention-guided mechanism. The module consists of three networks. The first network, caption-level context modeling, produces a 64-dimensional global context-enhanced features whereas the second network produces a 1024-dimensional regional context-enhanced features. The final network aggregates the contextual features and finds an optimal representation of it.

word-region interaction and global image-caption associations. In this study, we propose a contextual feature aggregation module (CFAM) that applies cross-modal feature interactions in two different granularities: word and caption. The block diagram of the proposed CFAM is illustrated in Figure 4.

### 3.4.1 Linear Fusion

First, we concatenate the global image features  $\mathbf{v} \in \mathbb{R}^{512}$  and the caption embeddings  $\mathbf{c} \in \mathbb{R}^{64}$  from the convolution-based projected head. Thus, we have a joint 576-dimensional multimodal representation. We then apply a fully connected (FC) layer. This network serves as a fusion scheme for our baseline approach.

### 3.4.2 Word-Level Context Modeling

In this network, we apply fine-grained cross-modal interactions between local image features and word embeddings. Here, we use word embeddings as cues to attend to the local image features extracted from the ArcFace FR module. We also experimented with using image features as cues to attend to words. However, that did not improve the performance, as words in a caption contain more abstract information than image regions. Figure 4 illustrates the word-level context modeling.

The inputs to the network are the word embeddings matrix,  $W \in \mathbb{R}^{L \times 64}$ , and local image features  $I \in \mathbb{R}^{256 \times 14 \times 14}$ . Batch normalization [12] is applied to the image features, before feeding it to a convolution layer of 64 filters with a kernel of size 3, and padding of 2. A max-pooling layer with a stride of size 2 is applied to the features map to reduce the spatial size to  $64 \times 8 \times 8$ . Next, a self-attention layer with a scale = 0.5 is applied to increase the intra-modality relationship among the local image features, followed by layer normalization [1].

Thus, due to the application of self-attention, each image region now contains information about the whole image. In

the self-attention layer, the *keys*, *queries*, and *values* are learned from  $1 \times 1$  convolutions. However, the number of filters in  $1 \times 1$  convolutions for projecting *key* and *query* are the multiplication of a *scale* factor of the number filters of the  $1 \times 1$  convolution for learning *values*. Note that the application of normalization and self-attention in this network, as analyzed in Table 3, is very crucial.

Contrary to image features, word embeddings  $W$ , have different dimensions. Therefore, we, first, calculate the correlation of the word embeddings matrix,  $W^T W \in \mathbb{R}^{64 \times 64}$ . Next, we reshape the embeddings matrix to size  $64 \times 8 \times 8$ . Similar to image features, we also experimented to implement self-attention to the reconstructed word features, but that does not improve the performance. The reason for this could be that as textual features are extracted from transformer-based BERT architectures, the intra-modal relationship among the features is already high. Afterward, the word embeddings and image features are fed into a cross-attention scheme to increase the inter-modality relationship. Here, the *queries* are learned from the word embeddings matrix, and *keys* and *values* are learned from the image features using  $1 \times 1$  convolutions with a *scale* of 0.5. Finally, after applying another max-pooling layer, we flatten the feature matrix to produce a 1024-dimensional output.

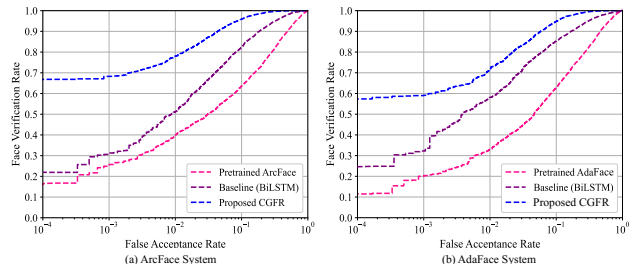
### 3.4.3 Caption-Level Context Modeling

Similar to the word level of granularity, we take the caption embedding as cues to attend to the global image features. Multi-head cross-attention has been employed to explore inter-modal associations between global image features and caption embedding. First, we reshape the global features into  $\mathbf{v} \in \mathbb{R}^{8 \times 64}$ . Then, we calculate the *queries* from caption embedding,  $\mathbf{c} \in \mathbb{R}^{64}$  and the *keys*, and *values* from global features  $\mathbf{v}$  using linear projection. The output of the cross-attention is a 64-dimensional vector, which is followed by a layer normalization [1].

594  
595  
596  
597  
598  
599  
600  
601  
602  
603  
604  
605  
606  
607  
608  
609  
610  
611  
612  
613  
614  
615  
616  
617  
618  
619  
620  
621  
622  
623  
624  
625  
626  
627  
628  
629  
630  
631  
632  
633  
634  
635  
636  
637  
638  
639  
640  
641  
642  
643  
644  
645  
646  
647

648 Table 1. The 1:1 verification and 1:N identification (Rank-1) re-  
 649 sults of our CGFR framework with ArcFace trained on the MM-  
 650 CelebA dataset. The top row represents the results of ArcFace  
 651 when pre-trained on MS1MV3 dataset [3].

Architectures	ROC Curve		TPR@FPR		Id(%)
	AUC	EER	1e-4	1e-3	
Pre-trained ArcFace [2]	85.27	23.48	16.75	25.73	17.56
Baseline	93.98	13.50	21.92	31.28	38.78
CGFR	<b>98.51</b>	<b>6.65</b>	<b>66.83</b>	<b>68.28</b>	<b>67.65</b>



658 Figure 5. ROC curves of 1:1 verification protocol of the proposed  
 659 CGFR framework with (a) ArcFace, (b) AdaFace FR module.

### 660 3.4.4 Features Aggregation Network

661 At the final stage of CFAM, we aggregate the contextualized  
 662 features from the word-level CM and caption-level  
 663 CM. Finally, a dense layer learns the optimal representation  
 664 in a joint multimodal feature space. In our experiment,  
 665 we found that the optimal dimension of the dense layer is  
 666 768. We also experimented to implement the CFAM module  
 667 on the textual features extracted from the BiLSTM text  
 668 encoder. However, it does not perform well as we failed  
 669 to obtain the contextual embeddings from the BiLSTM en-  
 670 coder.

## 671 3.5. Training Strategy

672 We train our proposed framework in two phases. First,  
 673 we train the TFRM module to update the contextual embed-  
 674 dings of the text encoder using the objective function men-  
 675 tioned in Equation 3. We finetune the BERT encoder for  
 676 only 4 epochs and use a mini-batch AdamW optimizer [23]  
 677 with a weight decay of 0.02. The learning rate is initialized  
 678 to 0.00001 and is warmed up to 0.0001 after 2,000 training  
 679 iterations. We then decrease it using the cosine decay strat-  
 680 egy [22] to 0.00001. The batch size is set to 16. For the pro-  
 681 jection head of both visual and textual streams, we employ  
 682 the Adam optimizer [15] with  $\beta_1 = 0.5$  and  $\beta_2 = 0.99$ . The  
 683 initial learning rate, in this case, is set to 0.001. In the sec-  
 684 ond phase, we train the whole framework end-to-end for 24  
 685 more epochs. However, the text encoder and the projection  
 686 head were trained with a similar setup to the first phase ex-  
 687 cept with a lower learning rate. Note that, in all the phases,  
 688 the parameters of the FR module were fixed.

702 Table 2. The 1:1 verification and 1:N identification (Rank-1) re-  
 703 sults of our CGFR framework with AdaFace trained on the MM-  
 704 CelebA dataset. The top row represent the results of AdaFace  
 705 when pre-trained on the WebFace4M dataset [42].

Architectures	ROC Curve		TPR@FPR		Id(%)
	AUC	EER	1e-4	1e-3	
Pre-trained AdaFace [14]	85.55	22.88	11.46	20.00	8.45
Baseline	93.97	12.88	24.28	33.00	22.55
CGFR	<b>98.10</b>	<b>7.52</b>	<b>58.08</b>	<b>59.12</b>	<b>53.23</b>

## 712 4. Experiments

### 713 4.1. Dataset

714 The Multit-Modal CelebA-HQ [33] (MMCelebA) is a  
 715 large-scale text-to-face dataset, originally built for face im-  
 716 age generation and facial attributes editing. It has a total of  
 717 30,000 high-resolution face images from the CelebA-HQ  
 718 dataset [21]. The dataset is split between 24,000 training  
 719 images and 6,000 test images. Each image has 10 auto-  
 720 generated captions from a total of 38 facial attributes.

### 721 4.2. Preprocessing

722 First, we implement standard data augmentation tech-  
 723 niques such as random sub-sampling, color jittering, hori-  
 724 zontal flipping, rotation, and Gaussian noise to degrade the  
 725 image quality of the MMCelebA dataset. Then, we resize  
 726 all the images to 3 x 112 x 112. Sample preprocessed im-  
 727 ages are shown in the Figure 1. The top row of Table 1  
 728 and Table 2 represent the performance of the pre-trained  
 729 ArcFace and AdaFace models on this preprocessed dataset,  
 730 respectively. From these tables, we observe that the per-  
 731 formance of both the pre-trained ArcFace and AdaFace mod-  
 732 els substantially degraded due to the poor generalization on  
 733 the low-quality images, which adversely affects their facial  
 734 analysis procedure [41].

### 735 4.3. Implementation

736 We implemented our architecture using two NVIDIA Ti-  
 737 tan RTX GPUs. In our experiment, we empirically set the  
 738 hyper-parameters in Equations 3 as follows:  $\lambda_1 = 1$ , and  $\lambda_2$   
 739 = 0.5. Since we employ pre-trained encoders, training the  
 740 proposed framework is very fast. Finetuning BERT for 4  
 741 epochs takes approximately 80 minutes on the MMCelebA  
 742 dataset while training the whole network end-to-end takes  
 743 8 hours. Also, due to the parallel strategy of our proposed  
 744 framework, the model has a very low time complexity dur-  
 745 ing inference. The inference time, which requires only one  
 746 forward process, is 220ms for an image-caption pair.

### 747 4.4. Performance Evaluation

748 **ArcFace System:** We compare our proposed CGFR to the  
 749 pre-trained ArcFace and the baseline approach, as shown

756 Table 3. Ablation experiments of different networks on the CFAM  
 757 module. Experimental results verifies the notion of fusing cross-  
 758 modal features at multiple granularities improves 1:1 VR(%).

Modules	ROC Curve		TPR@FPR	
	AUC	EER	1e-4	1e-3
w/o modules	89.96	18.27	15.95	21.42
Word (w/o Norm)	86.36	22.27	8.63	20.63
Word (w/o SA)	96.30	10.42	27.02	33.13
Word (SA+Norm)	96.86	9.88	53.42	54.45
Word + Caption	97.22	9.38	63.75	64.42
Word + Caption + FAN	<b>98.51</b>	<b>6.65</b>	<b>66.83</b>	<b>68.28</b>

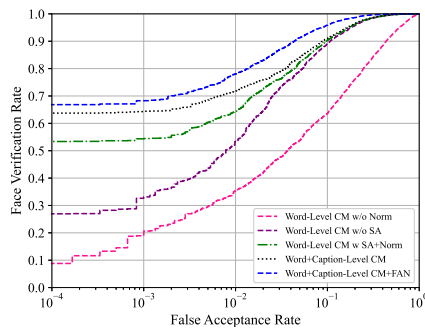
768 in Table 1. Our baseline is a dual-stream model employing  
 769 a BiLSTM text encoder with a linear fusion. In the  
 770 1:1 verification protocol, the proposed CGFR achieves the  
 771 highest verification rates (VR). It improved the pre-trained  
 772 ArcFace by 71.68% and the baseline by 50.74% on the  
 773 equal error rate (EER) metric. Also, using the true positive  
 774 rate (TPR) and false positive rate (FPR) metrics, as ill-  
 775 trated in Figure 5(a), our proposed CGFR improves the  
 776 VR(%) by a significant margin. In particular, as compared  
 777 to the pre-trained ArcFace model, our framework boosts  
 778 TPR(@FPR=1e-4) from 16.75% to 66.83%.

779 Similarly, when compared to the baseline approach, our  
 780 framework improves the TPR(@FPR=1e-4) from 21.92%  
 781 to 66.83% and TPR(@FPR=1e-3) from 31.28% to 68.28%.  
 782 Furthermore, in the 1:N identification protocol, the pro-  
 783 posed CFGR secures an improvement of 74.44% and  
 784 285.25% on Rank-1 identification accuracy over baseline  
 785 and pre-trained ArcFace, respectively. Therefore, as the  
 786 results show, the ArcFace FR module, which performs poorly  
 787 due to low quality and noise, could be significantly im-  
 788 proved using natural language supervision.

790 **AdaFace System:** In Table 2, we conduct further experiments  
 791 to evaluate the performance of our CGFR framework with an AdaFace FR module. As illustrated in Figure  
 792 5(b), our framework significantly improves the VR(%) over the baseline and pre-trained AdaFace. It improves  
 793 the pre-trained AdaFace by 67.13% and the baseline by 41.61%  
 794 on the EER metric. Also, in 1:1 verification protocol, under  
 795 the evaluation metric of TPR(@FPR=1e-4), our framework  
 796 boosts the performance of pre-trained AdaFace from  
 797 11.46% to 58.08% and TPR(@FPR=1e-3) from 20.00% to  
 798 59.12%. Furthermore, as reported in Table 2, the Rank-1  
 799 identification accuracy of our CGFR framework improves  
 800 by 136.05% over the baseline. Thus, the VR (%) of the  
 801 above-mentioned experiments proves the effectiveness and  
 802 generalizability of the proposed framework.

#### 803 4.5. Analysis of CFAM

804 We design an ablation experiment to evaluate the ef-  
 805 fectiveness of the proposed CFAM module. Specifically,



806 Figure 6. Face verification evaluation on different modules of the  
 807 proposed CFAM using ROC curves. Verification rates (%) illus-  
 808 trates the need for fusing contextual features in both word-level  
 809 and caption-level granularities.

810 we analyze the role of individual granularities and atten-  
 811 tion schemes. Table 3 demonstrates that a fusion scheme  
 812 without any granularity decreases the VR(%) and proves  
 813 the need for fusing contextual features at multiple granu-  
 814 larities. In fact, under the evaluation metric of TPR, word-  
 815 level contextual modeling (CM) increases the performance  
 816 by 234.92% (@FPR=1e-4) over the simple concatenation  
 817 of multimodal features. However, the choice of adding  
 818 normalization [12, 1] and self-attention are crucial to the  
 819 performance of this module. We observe a drastic per-  
 820 formance drop of 12.15% in AUC without normalization (one  
 821 batch norm [12] and two-layer norm [1]). Also, adding  
 822 self-attention to the image features reduces the EER from  
 823 10.42% to 9.88%.

824 We also observe that the fusion of word-level and  
 825 caption-level CM improves the VR(%) by 5.06% on EER  
 826 and 19.34% on TPR@FPR=1e-4 compared to word-level  
 827 CM. Furthermore, the ablation study shows that the im-  
 828 plementation of the feature aggregation network further  
 829 boosts the VR(%), improving TPR from 63.75% to 66.83%  
 830 (@FPR=1e-4). Figure 6 depicts the performance compar-  
 831 ison of these networks on ROC curves. Figure 6 illus-  
 832 trates that the proposed CFAM, with both CM networks  
 833 and the feature aggregation network, achieves the high-  
 834 est VR(%), proving the effectiveness of applying fine-grain  
 835 word-region and image-caption interaction.

## 836 5. Conclusion

837 We have introduced a new framework, called the  
 838 caption-guided face recognition (CGFR) model, to improve  
 839 the performance of FR systems using textual descriptions.  
 840 Our framework is based on a dual-stream model with a tex-  
 841 tual feature refinement module (TFRM), and a contextual  
 842 feature aggregation module (CFAM). CFAM applies fine-  
 843 grained cross-modal feature interaction at multiple granu-  
 844 larities using cross-attention. In contrast, TFRM helps the

864 framework to learn an effective joint multimodal embedding  
 865 space by realigning the text embeddings with visual  
 866 features. Our CGFR has significantly improved the perfor-  
 867 mance of two FR models. It has also enhanced the robust-  
 868 ness and reliability of the FR systems by offering higher  
 869 resistance to spoofing attacks. In the future, we aim to em-  
 870 ploy large-scale face image-caption pair datasets to assess  
 871 the generalizability of our proposed method.

## References

[1] J. L. Ba, J. R. Kiros, and G. E. Hinton. Layer normalization. *arXiv preprint arXiv:1607.06450*, 2016.

[2] J. Deng, J. Guo, N. Xue, and S. Zafeiriou. ArcFace: additive angular margin loss for deep face recognition. In *IEEE Conference on Computer Vision and Pattern Recognition*, pages 4685–4694, 2019.

[3] J. Deng, J. Guo, D. Zhang, Y. Deng, X. Lu, and S. Shi. Lightweight face recognition challenge. In *IEEE International Conference on Computer Vision Workshops*, pages 2638–2646, 2019.

[4] J. Devlin, M.-W. Chang, K. Lee, and K. Toutanova. BERT: Pre-training of deep bidirectional transformers for language understanding. In *North American Chapter of the Association for Computational Linguistics*, pages 4171–4186, 2019.

[5] E. Gonzalez-Sosa, J. Fierrez, R. Vera-Rodriguez, and F. Alonso-Fernandez. Facial soft biometrics for recognition in the wild: Recent works, annotation, and COTS evaluation. *IEEE Transactions on Information Forensics and Security*, 13(8):2001–2014, 2018.

[6] I. Goodfellow, J. Pouget-Abadie, M. Mirza, B. Xu, D. Warde-Farley, S. Ozair, and et al. Generative adversarial nets. In *Neural Information Processing Systems*, 2014.

[7] M. Guillaumin, T. Mensink, J. Verbeek, and C. Schmid. Face recognition from caption-based supervision. *International Journal of Computer Vision*, 96(1):64–82, 2012.

[8] K. He, X. Zhang, S. Ren, and J. Sun. Deep residual learning for image recognition. In *IEEE Conference on Computer Vision and Pattern Recognition*, pages 770–778, 2016.

[9] Z. He, W. Zuo, M. Kan, S. Shan, and X. Chen. AttGAN: Facial attribute editing by only changing what you want. *IEEE Transactions on Image Processing*, 28(11):5464–5478, 2019.

[10] S. Hochreiter and J. Schmidhuber. Long short-term memory. *Neural computation*, 9(8):1735–1780, 1997.

[11] Q. Huang, L. Yang, H. Huang, T. Wu, and D. Lin. Caption-supervised face recognition: Training a state-of-the-art face model without manual annotation. In *European Conference on Computer Vision*, pages 139–155, 2020.

[12] S. Ioffe and C. Szegedy. Batch normalization: Accelerating deep network training by reducing internal covariate shift. In *International conference on machine learning*, pages 448–456. pmlr, 2015.

[13] D. B. J. Lu, D. Parikh, and S. Lee. ViLBERT: Pretraining task-agnostic visiolinguistic representations for vision-and-language tasks. *Advances in neural information processing systems*, 32, 2019.

[14] M. Kim, A. K. Jain, and X. Liu. AdaFace: Quality adaptive margin for face recognition. In *IEEE Conference on Computer Vision and Pattern Recognition*, pages 18750–18759, 2022.

[15] D. P. Kingma and J. Ba. Adam: A method for stochastic optimization. *arXiv preprint arXiv:1412.6980*, 2014.

[16] K.-H. Lee, X. Chen, G. Hua, H. Hu, and X. He. Stacked cross attention for image-text matching. In *European conference on computer vision*, pages 201–216, 2018.

[17] J. Li, R. Selvaraju, A. Gotmare, S. Joty, C. Xiong, and S. C. H. Hoi. Align before fuse: Vision and language representation learning with momentum distillation. *Advances in neural information processing systems*, 34:9694–9705, 2021.

[18] S. Li, T. Xiao, H. Li, W. Yang, and X. Wang. Identity-aware textual-visual matching with latent co-attention. In *IEEE International Conference on Computer Vision*, pages 1908–1917, 2017.

[19] W. Li, C. Gao, G. Niu, X. Xiao, H. Liu, J. Liu, H. Wu, and H. Wang. UNIMO: Towards unified-modal understanding and generation via cross-modal contrastive learning. *Proceedings of the 59th Annual Meeting of the Association for Computational Linguistics*, pages 2592–2607, 2021.

[20] Y. Liu, M. Ott, N. G., J. Du, M. Joshi, D. Chen, O. Levy, M. Lewis, L. Zettlemoyer, and V. Stoyano. RoBERTa: A robustly optimized bert pretraining approach. *CoRR*, abs/1907.11692, 2019.

[21] Z. Liu, P. Luo, X. Wang, and X. Tang. Deep learning face attributes in the wild. In *IEEE International Conference on Computer Vision*, pages 3730–3738, 2015.

[22] I. Loshchilov and F. Hutter. SGDR: stochastic gradient descent with warm restarts. In *International Conference on Learning Representations*, 2017.

[23] I. Loshchilov and F. Hutter. Decoupled weight decay regularization. In *International Conference on Learning Representations*, 2019.

[24] K. Niu, Y. Huang, W. Ouyang, and L. Wang. Improving description-based person re-identification by multi-granularity image-text alignments. *IEEE Transactions on Image Processing*, 29:5542–5556, 2020.

[25] A. Radford, J. Kim, C. Hallacy, A. Ramesh, G. Goh, S. Agarwal, and et al. Learning transferable visual models from natural language supervision. In *International Conference on Machine Learning*, pages 8748–8763, 2021.

[26] V. Sanh, L. Debut, J. Chaumond, and T. Wolf. DistilBERT, a distilled version of BERT: smaller, faster, cheaper and lighter. *arXiv preprint arXiv:1910.01108*, 2019.

[27] M. Schuster and K. Paliwal. Bidirectional recurrent neural networks. *IEEE Transactions on Signal Processing*, 45(11):2673–2681, 1997.

[28] H. Shi, H. Li, F. Meng, and Q. Wu. Key-word-aware network for referring expression image segmentation. In *Proceedings of the European Conference on Computer Vision*, 2018.

[29] J. Sun, Q. Deng, Q. Li, M. Sun, M. Ren, and Z. Sun. AnyFace: Free-style text-to-face synthesis and manipulation. In *IEEE Conference on Computer Vision and Pattern Recognition*, pages 18687–18696, 2022.

972 [30] P. Tome, J. Fierrez, R. Vera-Rodriguez, and M. S. Nixon. 1026  
 973 Soft biometrics and their application in person recognition at 1027  
 974 a distance. *IEEE Transactions on Information Forensics and 1028  
 975 Security*, 9(3):464–475, 2014. 1029  
 976 [31] A. Vaswani, N. Shazeer, N. Parmar, J. Uszkoreit, L. Jones, 1030  
 977 A. N. Gomez, and et al. Attention is all you need. *Advances 1031  
 978 in neural information processing systems*, 30, 2017. 1032  
 979 [32] T. Wang, T. Zhang, and B. Lovell. Faces à la Carte: Text- 1033  
 980 to-face generation via attribute disentanglement. In *2021 1034  
 981 IEEE Winter Conference on Applications of Computer 1035  
 982 Vision*, pages 3379–3387, 2021. 1036  
 983 [33] W. Xia, Y. Yang, J.-H. Xue, and B. Wu. TediGAN: Text- 1037  
 984 guided diverse face image generation and manipulation. In 1038  
 985 *IEEE Conference on Computer Vision and Pattern 1039  
 986 Recognition*, pages 2256–2265, 2021. 1040  
 987 [34] B. Xu, N. Wang, T. Chen, and M. Li. Empirical evaluation of 1041  
 988 rectified activations in convolutional network. *arXiv preprint 1042  
 989 arXiv:1505.00853*, 2015. 1043  
 990 [35] K. Xu, J. Ba, R. Kiros, K. Cho, A. Courville, R. Salakhudinov, 1044  
 991 and et al. Show, attend and tell: Neural image caption 1045  
 992 generation with visual attention. In *International conference 1046  
 993 on machine learning*, pages 2048–2057, 2015. 1047  
 994 [36] T. Xu, P. Zhang, Q. Huang, H. Zhang, Z. Gan, X. Huang, and 1048  
 995 X. He. AttnGAN: Fine-grained text to image generation with 1049  
 996 attentional generative adversarial networks. In *IEEE Conference 1050  
 997 on Computer Vision and Pattern Recognition*, pages 1316–1324, 2018. 1051  
 998 [37] L. Ye, M. Rochan, Z. Liu, and Y. Wang. Cross-modal self- 1052  
 999 attention network for referring image segmentation. In *IEEE 1053  
 1000 Conference on Computer Vision and Pattern Recognition*, 1054  
 1001 pages 10494–10503, 2019. 1055  
 1002 [38] X. Yin, Y. Tai, Y. Huang, and X. Liu. FAN: Feature 1056  
 1003 adaptation network for surveillance face recognition and 1057  
 1004 normalization. In *Asian Conference on Computer Vision*, 2020. 1058  
 1005 [39] H. Zhang, J. R. Beveridge, B. A. Draper, and P. J. Phillips. 1059  
 1006 On the effectiveness of soft biometrics for increasing face 1060  
 1007 verification rates. *Computer Vision and Image Understanding*, 1061  
 1008 137:50–62, 2015. 1062  
 1009 [40] Y. Zhang and H. Lu. Deep cross-modal projection learning 1063  
 1010 for image-text matching. In *European conference on computer 1064  
 1011 vision (ECCV)*, pages 686–701, 2018. 1065  
 1012 [41] S. Zhu, S. Liu, C. C. Loy, and X. Tang. Deep cascaded bi- 1066  
 1013 network for face hallucination. In *European conference on 1067  
 1014 computer vision*, pages 614–630, 2016. 1068  
 1015 [42] Z. Zhu, G. Huang, J. Deng, Y. Ye, J. Huang, X. Chen, and 1069  
 1016 et al. Webface260m: A benchmark unveiling the power 1070  
 1017 of million-scale deep face recognition. In *IEEE Conference 1071  
 1018 on Computer Vision and Pattern Recognition*, pages 10492– 1072  
 1019 10502, 2021. 1073  
 1020  
 1021  
 1022  
 1023  
 1024  
 1025